PERFORMANCE DEGRADATION ANALYSIS OF COMBINED CYCLE POWER PLANT UNDER HIGH AMBIENT TEMPERATURE

by

Anping WAN[a,b] and Ting CHEN[a,b*]

[a] Department of Engineering, Zhejiang University City College, Hangzhou, China
[b] Key Laboratory of Urban Rail Transit Intelligent Operation and Maintenance Technology & Equipment of Zhejiang Province, Zhejiang Normal University, Jinhua, China

Original scientific paper
https://doi.org/10.2298/TSCI210221226W

The mechanism of performance degradation of a natural gas combined cycle power plant under high ambient temperature is studied by analysing the performance characteristics and thermal properties of the working fluids. Real operating data under typical seasonal conditions are collected and studied. The results reveal that the power output of the natural gas combined cycle system decreases by 22.6%, and the energy efficiency decreases from 57.28-56.3% when the ambient temperature increases from 5-35 °C. Gas turbine total power output and steam turbine power output decrease by 17.0% and 16.2%, respectively, as ambient temperature increases from 5-35 °C. The enthalpy difference of the flue gas between the turbine inlet and outlet change slightly with varying ambient temperature. The fuel and air input decrease by 16.0% and 16.2%, respectively, as ambient temperature increases from 5-35 °C. By analysing the calculated results, the decrement in air and fuel input d is considered as the immediate cause of system power output reduction. The proportion of power consumed by air compressor reaches 50.4% at 35 °C. This is considered to be caused by air compressor idle.

Key words: *natural gas combined cycle, performance degradation, enthalpy, ambient temperature*

Introduction

With the increasing demand for electric power and awareness for environment protection, the development of power generation technologies has been moving to the direction of high power output and clean production [1-5]. Power generation by using clean energy sources, such as solar energy, wind energy, and geothermal energy are more environmentally friendly than fossil fuel, and they have been becoming more and more important [6-10]. However, clean energy sources are highly depended on the local natural conditions and local natural resources. By now, fossil fuel is still the main energy source for power generation. In China, about 90% of the electricity is generated from hydro-power plant and coal-power plant [11].

* Corresponding author, e-mail: chenting@zucc.edu.cn

Natural gas combined cycle (NGCC) power plants that use gas turbines (GT) and steam turbines (ST) have been attracted great attention due to their high efficiency and short start-up time [12-14].

Although natural gas-based power plant only accounts for about 5% in China, it tends to increase in a long period. Thermal performance investigations on NGCC power plants have been carried on actively [15-22]. The ambient temperature is an important factor that has a considerable effect on the thermal performance of an NGCC power plant. Sen *et al.* [23] investigated the thermal performance of an NGCC power plant in Turkey in the ambient temperature range of 8-23 °C. The results reveal that the electricity production and efficiency of the GT decrease with the increase in the ambient temperature, and an air cooling system is recommended to increase the electricity production and efficiency. Hashmi *et al.* [24] studied the combined effect of inlet air cooling and fouling on the performance of industrial turbines. They concluded that both of the inlet air temperature has a great impact on the thermal performance of GT. By applying reheating, recuperation, and coolant inter-cooling on the GT, Kwon *et al.* [25] investigated the performance enhancement of a combined cycle power plant (CCPP). Yazdi *et al.* [26] compared the effects of using absorption chiller, heat pump, and inlet fogging systems for cooling the inlet air of a GT power plant for four cities in Iran under different climate conditions. The results showed that the inlet air cooling systems is effective in increasing the power output. In warm and dry climates, the absorption chiller system and the inlet fogging system exhibit the best performance. In the humid climates, the heat pump system is recommended. Liu *et al.* [27] investigated the performance of a power plant with a novel inlet air cooling system. They revealed that when the power plant with novel air cooling system produces 1.8-14.4% higher power output than that without inlet air cooling for inlet air temperatures ranging between 28 °C and 40 °C.

Although the conclusion that the higher ambient temperature will lead to a degradation in the performance of NGCC power plant has been widely accepted, the mechanism of the degradation is stilled needed to be further investigated and revealed. In the existing literature, only the power output variation with weather conditions are displayed, there are few results about the variations of the flue gas properties and efficiencies of different components can be found. In this study, an NGCC power plant in Hangzhou, China, is investigated. The site figure of the power plant is shown in fig. 1. In addition to the system performance variations with weather conditions, the thermal properties of the flue gas at the inlet and outlet of the turbine are calculated and analyzed to help us to achieve better comprehension about the system performance degradation.

Figure 1. The studied NGCC power plant in Hangzhou, China

Instructions

The NGCC power plant system

In this study, an NGCC power plant located in Hangzhou, China, is studied. This system consists of a PG9351FA GT, a triple-pressure heat recover steam generator (HRSG), a D10 ST, and a 390H hydrogen-cooled generator. The specifications and operation conditions of the NGCC power plant are listed in tab. 1. Compared with the ambient temperature, the effect of the relative humidity on the performance of NGCC power plant is small [23, 24], and the relative humidity in Hangzhou city changes little with season. Due to this reason, only the effect of the ambient temperature on the NGCC power plant performance is investigated. The blocks of the studied NGCC power plant system are illustrated in fig. 2. As shown in this figure, part of the compressed air enters the turbine to cool the blade so that the turbine can be operated under bearable temperature, and the percentage of the cooling air is approximately 18%.

The operating state of the NGCC power plant system is monitored by using distribute control system (DCS) that is connected with transmitters installed in relevant nodes of the plant. The data is transferred to supervisory information system (SIS) and saved in the plant information real-time database.

The main performance indicators of a CCPP are power output, P, and total thermal efficiency, η_{NGCC}.

The power output is calculated:

$$P = P_{\mathrm{GT}} + P_{\mathrm{ST}} \tag{1}$$

where P_{GT} is the net power generation of GT, and P_{ST} is the power output of ST.

The energy efficiency of the system is:

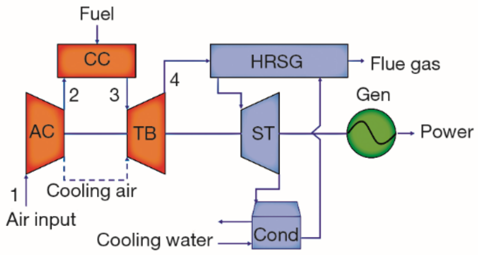

Figure 2. Schematic of the NGCC power plant system

Table 1. Specifications and operation conditions of the NGCC power plant

Parameter	Value
Inlet air temperature, [°C]	5~35
AC revolution speed, [rpm]	3000
Cooling water inlet temperature, [°C]	13~31.8
AC pressure ratio, γ	15.4
AC efficiency	0.9
CC efficiency	0.9
ST efficiency	0.9
Turbine efficiency	0.95
HRSG efficiency	0.8

$$\eta_{\mathrm{NGCC}} = 3.6 \frac{P}{M_{\mathrm{ng}} LHV \eta_{\mathrm{CC}}} \tag{2}$$

where η_{CC} is combustion efficiency.

The NGCC power plant system

To understand the performance degradation of the NGCC system, it is necessary to calculate the thermal properties of working fluid at different positions accurately. In this study, the calculation is carried out by taking all the constituents in the working fluid into consideration. The constituents and properties of natural gas used in the present NGCC power plant are listed in tab. 2. The lower heating value (LHV) of the natural gas is 48625 kJ/kg.

The specific heat of different compositions in the flue gas can be calculated:

$$c_p = c_p(T) = \sum_{i=1}^{9} \left[a_{c,i} \left(\frac{T}{1000} \right)^i \right] \tag{3}$$

The specific enthalpy can be calculated:

$$h = h(T) = A_h + \sum_{i=1}^{9} \left[a_{h,i} \left(\frac{T}{1000} \right)^i \right] + B_h \ln\left(\frac{T}{1000} \right) \tag{4}$$

Table 2. Constituents and properties of natural gas

	Constituents	Compression factor, C_j	Volume ratio, V_j%	Molar ratio, X_j%
1	CH_4	0.9981	98.109	98.09773
2	C_2H_6	0.992	0.525	0.528168
3	C_3H_8	0.9834	0.057	0.057845
4	C_4H_{10}	0.9682	0.025	0.025769
5	C_5H_{12}	0.945	0.016	0.016897
6	C_{6+}	0.919	0.039	0.042352
7	N_2	0.9997	0.601	0.599969
8	CO_2	0.9944	0.629	0.631268

The specific entropy can be calculated:

$$s = s(T) = A_s + \sum_{i=1}^{9} \left[a_{s,i} \left(\frac{T}{1000} \right)^i \right] + B_s \ln\left(\frac{T}{1000} \right) \tag{5}$$

where $a_{c,i}$, A_h, $a_{h,i}$, B_h, A_s, $a_{s,i}$, B_s are constants.

The thermal properties of wet air and the flue gas can be calculated:

$$\psi_{\text{mix}} = \sum_{i=1}^{i} X_i \psi_i \tag{6}$$

where Ψ represents specific heat, specific enthalpy, or specific entropy, X – the molar ratio of each composition, and i represents different components.

Then the temperatures of the air and flue gas can be determined from the thermal properties:

$$T = T_h(h) = \begin{cases} T^{(1)} = \dfrac{h}{c_{p,600}} \\ h^{(i)} = h[T^{(i)}] \\ T^{(i+1)} = T^{(i)} + \dfrac{h - h^{(i)}}{c_{p,600}} \end{cases} \tag{7}$$

$$\ln \frac{P_{i+1}}{P_i} = \frac{s_{i+1} - s_i}{\mathrm{R}} \tag{8}$$

$$\pi = \frac{P_{i+1}}{P_i} \tag{9}$$

$$T = T_{\ln\pi}(\ln\pi) = \begin{cases} T^{(1)} = \exp\left(\dfrac{\mathrm{R}\ln\pi}{c_{p,200}}\right) \\ \ln\pi^{(i)} = \dfrac{s[T^{(i)}]}{\mathrm{R}} \\ T^{(i+1)} = T^{(i)} + \dfrac{\ln\pi^{(1)} - \ln\pi^{(i)}}{\dfrac{c_{p,T^{(i)}}}{\mathrm{R}T^{(i)}}} \end{cases} \tag{10}$$

The GT performance analysis

The isentropic efficiency and the power consumption of the air compressor are:

$$\eta_{\mathrm{AC}} = \frac{h_{2s} - h_1}{h_2 - h_1} \tag{11}$$

$$P_{\mathrm{AC}} = \frac{1000}{3600} M_{\mathrm{a}}(h_2 - h_1) \tag{12}$$

The isentropic efficiency and the total power output of the GT are:

$$\eta_{\mathrm{GT,s}} = \frac{h_3 - h_4}{h_3 - h_{4\mathrm{s}}} \tag{13}$$

$$P_{\mathrm{TB}} = \frac{1000}{3600} M_{\mathrm{a}}(h_3 - h_4) \tag{14}$$

Since part of the power that generated by the turbine is used to drive the AC, then the net power output of the GT is:

$$P_{\mathrm{GT}} = P_{\mathrm{TB}} + P_{\mathrm{AC}} \tag{15}$$

The ratio of the power consumption of AC to the power output of TB can be calculated:

$$f = \frac{P_{\mathrm{AC}}}{P_{\mathrm{TB}}} \tag{16}$$

The thermal efficiency of the GT is:

$$\eta_{\mathrm{GT,TB}} = 3.6 \frac{P_{\mathrm{GT}}}{M_{\mathrm{ng}} LHV \eta_{\mathrm{CC}}} \tag{17}$$

The ST performance analysis

The ST consists of an high pressure (HP) steam turbine, an intermediate pressure (IP), and an low pressure (LP) steam turbine. The isentropic efficiencies of the three steam turbines and the power generation of the ST are:

$$\eta_{\mathrm{ST,s}}^{h} = \frac{h_5^h - h_6^h}{h_5^h - h_{6\mathrm{s}}^h} \tag{18}$$

$$\eta^{i}_{\mathrm{ST,s}} = \frac{h^{i}_{5} - h^{h}_{6}}{h^{i}_{5} - h^{h}_{6\mathrm{s}}} \tag{19}$$

$$\eta^{l}_{\mathrm{ST,s}} = \frac{h^{l}_{5} - hl}{h^{l}_{5} - h^{l}_{6\mathrm{s}}} \tag{20}$$

$$P_{\mathrm{ST}} = \frac{1000}{3600} M_{\mathrm{f}} (h_5 - h_6) \tag{21}$$

where the superscript h, i, and l represent the HP steam turbine, IP steam turbine, and LP steam turbine, respectively.

Results and discussion

To verify the analysis model, the comparison of the power output of the experimental data and calculation results is shown in fig. 3. The analysis model is well matched with the practical data, the average difference is 2.43%. The results show that when the ambient temperature changes from 5-35 °C, the total power output of the NGCC system decreases by 22.6% from 433.16-335.21 MW, and the energy efficiency decreases from 57.28% to 56.3%.

To ensure a long stable operation of the GT, the inlet temperature of the turbine is controlled by adjusting mass-flow rates of fuel and air input and it is kept relative constant. The temperature variations of the flue gas at the inlet, T_3, and outlet, T_4, of the turbine with ambient temperature are displayed in fig. 4.

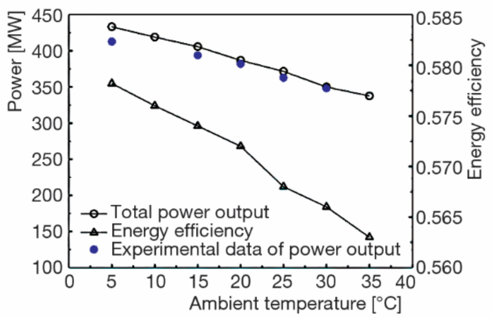

Figure 3. Variations of NGCC power output and energy efficiency

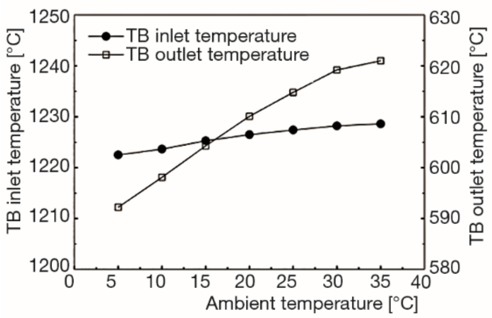

Figure 4. Variations of TB inlet and outlet temperature against ambient temperature

The variations net power output of GT, P_{GT}, the total power output of TB, P_{TB}, and the power output of ST, P_{ST}, with ambient temperature are given in fig. 5. When the ambient temperature changes from 5-35 °C, P_{TB}, P_{GT}, and P_{AC} decrease from 536.35-445.13 MW, 290.37-215.3 MW, and 141.9-118.9 MW, respectively. The decrease of the P_{TB}, P_{GT}, and P_{ST} is 17.01%, 24.9%, and 16.2%, respectively.

Figure 6 shows the variations isentropic efficiencies of different components with ambient temperature. The isentropic efficiency of turbine decreases as ambient temperature increases. However, the isentropic efficiency of AC increases at first, then decreases as ambient temperature increases, and its highest value of 0.87 is obtained when the temperature is 20 °C. The isentropic efficiencies of HP and IP almost keep constant with changing ambient temperature, and the isentropic efficiency of LP increases at first then decrease. In overall, the isentropic efficiencies of GT and ST changes slightly.

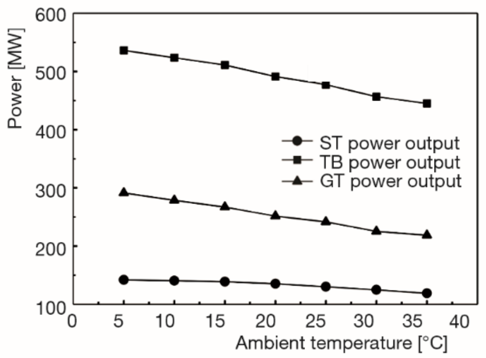

Figure 5. Variations of power output of ST, TB, and GT

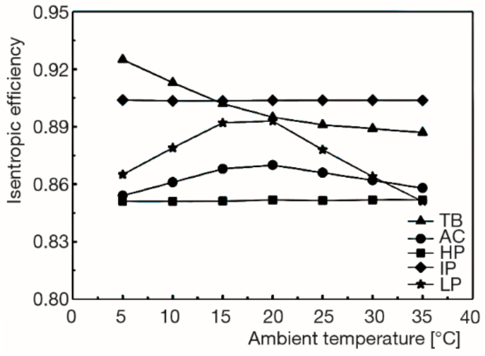

Figure 6. Variations of isentropic efficiency

The enthalpy variations of flue gas at the inlet and outlet of turbine are shown in fig. 7. When the ambient temperature changes from 5-35 °C, the flue gas enthalpy at the inlet and outlet increase from 48848.4 kJ/kmol to 49550 kJ/kmol and 26646.9 kJ/kmol to 27930.1 kJ/kmol, respectively. The difference in enthalpy between the inlet and outlet is almost kept constant with ambient temperature increase. It indicates that the power that generated by the GT is almost kept constant as temperature changes from 5-35 °C.

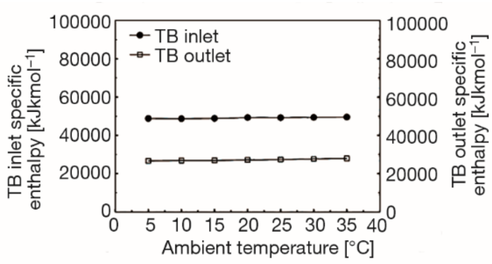

Figure 7. Variations of specific enthalpies of flue gas at TB inlet and outlet

The variations of air mass-flow rate and fuel input are shown in fig. 8. When the weather condition changes from 5-35 °C, the air mass-flow rate decreases by 16.4% and the fuel input decreases by 16.0%. As displayed in fig. 5, P_{GT} and P_{STt} decrease by 16.2% and 17.0%, respectively, as ambient temperature increases from 5-35 °C, which are extremely close to the decrease of fuel input and air input. It means that the power output decrease is mainly ascribed to the decrease in fuel and air input.

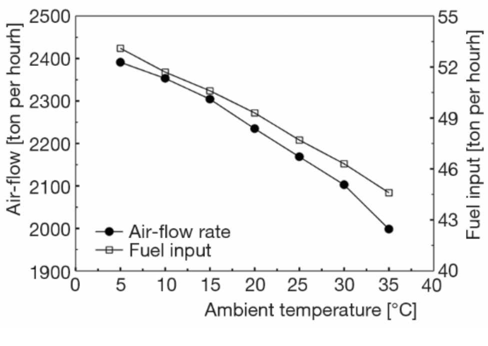

Figure 8. Variations of air-flow rate and fuel input rate

Figure 9 shows the variations of *f* and AC power consumption. The ratio of P_{AC} to P_{TB}. It can be seen that the AC power consumption decreases significantly as temperature increases, especially when the temperature is higher than 15 °C. However, the ratio of P_{AC} to P_{TB} increases slowly with increasing ambient temperature, and it reaches the highest value of 50.4% at 35 °C. The reason is that the AC rotating speed is kept constant at 3000 rpm, and it is inde-

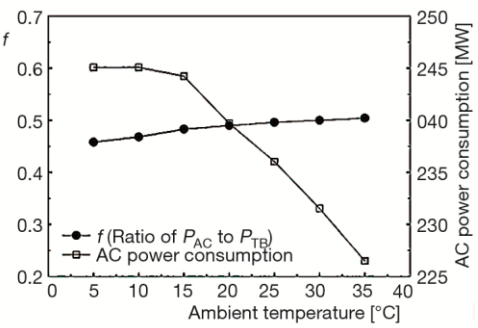

Figure 9. Variations of *f* and AC power consumption

pendent of the weather conditions, it means that the AC is idling high ambient temperature condition to some extent compared to that under low ambient temperature condition.

Conclusions

The performance an NGCC power plant in Hangzhou, China, depending on the ambient temperature variations is examined. The mechanism of system performance degradation under high ambient temperature is investigated by analyzing the thermal property variations of working fluids and the relationship between the power output and the fuel/air input. Considering that the humidity ratio in Hangzhou changes a lot with the seasons, which can have a considerable effect on the thermal property calculation, the thermal properties of the air and the flue gas are calculated according to their constituents.

The results show that power output of the NGCC power plant at 5 °C is 433.16 MW, while power output at 35 °C is 335.21 MW with a decrease of 22.6%. The reason for this reduction is that less fuel and air is compressed into the CC under high ambient temperature. The decrease proportions of the GT total power output and ST power output are very close to that of air and fuel input. The efficiencies of GT and ST change slightly as ambient temperature increases. Besides, the enthalpy difference between the inlet and outlet of the turbine is almost kept constant with the variation of ambient temperature. Thus, it can be concluded that the ambient temperature increase is not the essential cause that leads to the decrease in power output, air and fuel input reduction is the one. The energy efficiency of the system is 57.28% at 5 °C and 56.3% at 35 °C. The results reveal that the ratio of power consumed by AC to GT total power output is increased as ambient temperature increases. The reason is that the AC is kept rotating at a constant speed, less air is compressed under the high ambient condition, the AC is idle to some extent, and the GT efficiency is decreased.

Acknowledgment

This Research is Financially Supported by Scientific Research Foundation of Zhejiang University City College (No. J-202115).

Nomenclature

Cond – condenser, [–]
c_p – specific heat, [Jkg^{-1}K^{-1}]
Gen – generator, [–]
f – ratio of P_{ac} to P_t, [–]
LHV – lower heating value, [kJkg^{-1}]
h – specific enthalpy, [kJkmol^{-1}]
M – mass flow rate, [kgs^{-1}]
P – power output, [MW]
R – gas constant, [–]
s – entropy, [kJkmol^{-1}]
T – temperature, [°C]
X – molar ratio, [%]

Greek symbol

η – efficiency, [%]

Superscripts

h – high pressure steam turbine
i – intermediate pressure steam turbine
l – low pressure steam turbine

Subscripts

a – air
f – flue gas
mix – mixture

ng – natural gas
s – isentropic

Acronyms

AC – air compressor
Cond – condenser
CC – combustion chamber
CCPP – combined cycle power plant
Gen – generator
GT – gas turbine
HP – high pressure steam turbine
HRSG – heat recovery steam generator
IP – intermediate pressure steam turbine
LP – low pressure steam turbine
NGCC – natural gas combined cycle
ST – steam turbine
TB – turbine

References

[1] Sheibani, M. R., *et al.*, Economics of Energy Storage Options to Support a Conventional Power Plant: A Stochastic Approach for Optimal Energy Storage Sizing, *Journal of Energy Storage*, *33* (2020), Jan., 101892
[2] Adhami, H., Development and Thermoeconomic Analysis of a 250 MW Steam Power Plant by Gas Turbine, Photovoltaic, Photovoltaic/Thermal and Absorption Chiller, *Solar Energy*, *209* (2020), Oct., pp.123-134
[3] Romeo, L. M., *et al.*, Reducing Cycling Costs in Coal Fired Power Plants Through Power to Hydrogen, *International Journal of Hydrogen Energy, 45* (2020), 48, pp. 25838-25850
[4] Revathy, G., *et al.*, Optimization Study on Competence of Power Plant Using Gas/Steam Fluid Material Parameters by Machine Learning Techniques, *Materials Today: Proceedings, 37* (2021), 2, pp. 1713-1720
[5] Yazdani, S., *et al.*, A Comparison Between a Natural Gas Power Plant and a Municipal Solid Waste Incineration Power Plant Based on an Energy Analysis, *Journal of Cleaner Production, 274* (2020), Nov., 123158
[6] Khajepour, S, Ameri, M., Techno-Economic Analysis of a Hybrid Solar Thermal-PV Power Plant, *Sustainable Energy Technologies and Assessments, 42* (2020), Dec., 100857
[7] Simla, T., Stanek, W., Influence of the Wind Energy Sector on Thermal Power Plants in the Polish Energy System, *Renewable Energy, 161* (2020), Dec., pp. 928-938
[8] Mahmood, I., *et al.*, Modeling, Simulation and forecasting of Wind Power Plants Using Agent-Based Approach, *Journal of Cleaner Production, 276* (2020), Dec., 124172
[9] Wang, Y., *et al.*, Performance Analysis of an Improved 30 MW Parabolic Trough Solar Thermal Power Plant, *Energy, 213* (2020), Dec., 118862
[10] Heidarnejad, P., *et al.*, A Comprehensive Approach for Optimizing A Biomass Assisted Geothermal Power Plant with Freshwater Production: Techno-Economic and Environmental Evaluation, *Energy Conversion and Management, 226* (2020), Dec., 113514
[11] Kasumu, A. S., *et al.*, Country-Level Life Cycle Assessment of Greenhouse Gas Emissions from Liquefied Natural Gas Trade for Electricity Generation, *Environmental Science & Technology, 52* (2018), 4, pp. 1735-1746
[12] Meegahapola, L., Flynn, D., Characterization of Gas Turbine Lean Blowout During Frequency Excursions in Power Networks, *IEEE Transactions on Power Systems, 30* (2015), 4, pp. 1877-1887
[13] Xiang, Y., *et al.*, Study on the Configuration of Bottom Cycle in Natural Gas Combined Cycle Power Plants Integrated with Oxy-Fuel Combustion, *Applied Energy, 212* (2018), Feb., pp. 465-477
[14] Alobaid, F., Start-Up Improvement of a Supplementary-Fired Large Combined-Cycle Power Plant, *Journal of Process Control, 64* (2018), Apr., pp. 71-88
[15] Ibrahim, T. K. , *et al.*, Thermal Performance of Gas Turbine Power Plant Based on Exergy Analysis, *Applied Thermal Engineering, 115* (2017), Mar., pp. 977-985
[16] Chmielniak, T., *et al.*, Simulation Modules of Thermal Processes for Performance Control of CHP Plant with a Gas Turbine Unit, *Applied Thermal Engineering, 27* (2007), 13, pp. 2181-2187
[17] Yu, H., *et al.*, An Improved Combined Heat and Power Economic Dispatch Model for Natural Gas Combined Cycle Power Plants, *Applied Thermal Engineering, 181* (2020), Nov., 115939
[18] Patiño, E. G. G., Rivera, F. N., Global Warming Potential and Net Power Output Analysis of Natural Gas Combined Cycle Power Plants Coupled with CO_2 Capture Systems and Organic Rankine Cycles, *Journal of Cleaner Production, 208* (2019), Jan., pp. 11-18

[19] Kahraman, M., *et al.*, Thermodynamic and Thermoeconomic Analysis of a 21 MW Binary Type Air-Cooled Geothermal Power Plant and Determination of the Effect of Ambient Temperature Variation on the Plant Performance, *Energy Conversion and Management, 192* (2019), July, pp. 308-320
[20] Unal, F., Özkan, D. B., Application of Exergoeconomic Analysis for Power Plants, *Thermal Science, 22* (2017), 6A, pp. 2653-2666
[21] Alus, M., *et al.*, Optimization of the Triple-Pressure Combined Cycle Power Plant, *Thermal Science, 16* (2012), 3, pp. 901-914
[22] Xu, C., *et al.* Performance Improvement of a 330MWe Power Plant by Flue Gas Heat Recovery System, *Thermal Science 20* (2014), 1, pp. 303-314
[23] Sen, G., *et al.*, The Effect of Ambient Temperature on Electric Power Generation in Natural Gas Combined Cycle Power Plant – A Case Study. *Energy Reports, 4* (2018), Nov., pp. 682-690
[24] Hashmi, M. B., *et al.*, Combined Effect of Inlet Air Cooling and Fouling on Performance of Variable Geometry Industrial Gas Turbines, *Alexandria Engineering Journal, 59* (2020), 3, pp. 1811-1821
[25] Kwon, H. M., *et al.*, Performance Enhancement of the Gas Turbine Combined Cycle by Simultaneous Reheating, Recuperation, and Coolant Inter-Cooling, *Energy, 207* (2020), Sept., 118271
[26] Yazdi, M. R. M., *et al.*, Comparison of Gas Turbine Inlet Air Cooling Systems for Several Climates in Iran Using Energy, Exergy, Economic, and Environmental (4E) Analyses, *Energy Conversion and Management, 216* (2020), July., 112944
[27] Liu, Z., *et al.*, A Novel Inlet Air Cooling System Based on Liquefied Natural Gas Cold Energy Utilization for Improving Power Plant Performance, *Energy Conversion and Management, 187* (2019), May, pp. 41-52

Paper submitted: February 21, 2021
Paper revised: May 26, 2021
Paper accepted: May 27, 2021